Experimental Thermal and Fluid Science 34 (2010) 1475–1483

Contents lists available at ScienceDirect

Experimental Thermal and Fluid Science

journal homepage: www.elsevier.com/locate/etfs

Measuring air core characteristics of a pressure-swirl atomizer via a transparent acrylic nozzle at various Reynolds numbers

Eun J. Lee [a], Sang Youp Oh [a], Ho Y. Kim [a,*], Scott C. James [b], Sam S. Yoon [a]

[a] Dept. of Mechanical, Korea University Anamdong, 5-Ga, Sungbukgu, 136-713 Seoul, Republic of Korea
[b] Thermal/Fluid Science & Engineering, Sandia National Labs, PO Box 969, Livermore, CA 94551, United States

ARTICLE INFO

Article history:
Received 13 July 2009
Received in revised form 20 May 2010
Accepted 12 July 2010

Keywords:
Swirl spray
Temperature effect
Air core
Fuel injector performance

ABSTRACT

Because of thermal fluid-property dependence, atomization stability (or flow regime) can change even at fixed operating conditions when subject to temperature change. Particularly at low temperatures, fuel's high viscosity can prevent a pressure-swirl (or simplex) atomizer from sustaining a centrifugal-driven air core within the fuel injector. During disruption of the air core inside an injector, spray characteristics outside the nozzle reflect a highly unstable, nonlinear mode where air core length, Sauter mean diameter (SMD), cone angle, and discharge coefficient variability. To better understand injector performance, these characteristics of the pressure-swirl atomizer were experimentally investigated and data were correlated to Reynolds numbers (*Re*). Using a transparent acrylic nozzle, the air core length, SMD, cone angle, and discharge coefficient are observed as a function of *Re*. The critical Reynolds numbers that distinguish the transition from unstable mode to transitional mode and eventually to a stable mode are reported. The working fluids are diesel and a kerosene-based fuel, referred to as bunker-A.

1. Introduction

Pressure-swirl (or simplex) atomizers are used in many agricultural, chemical, industrial, and commercial applications, such as insecticide application, spray drying [1], cooling [2,3], painting, fuel injected engines [4–7], aircraft turbine engines [8–10], sprinklers, and fire suppression systems. Particularly, pressure-swirl injectors are widely used in aircraft internal combustion engines because of their inherent simplicity, high atomization performance, and reliable combustion stability [10]. As evident in its name, a pressure-swirl injector is characterized by the helical rotation of fuel through the injector nozzle.

In a swirl atomizer, fuel is supplied to the nozzle chamber along a tangential entry port that, under sufficient centrifugal force, yields a strong vortex (or swirl motion), which sustains an air core inside the chamber; see Fig. 1a. The stability of this air core (i.e., constant shape and height) is one of the most important performance metrics of swirl atomizers. Designs are often based on a classical air column stability analysis is found [11,12], who identify the most unstable wavelength (λ) at the free surface of a rotating air column as 6.48 times the column diameter.

Along with a stable air core, film thickness and spray cone angle are also important parameters that determine the performance of a simplex atomizer. A thinner fuel film (or sheet) results from a stronger vortex and yields smaller atomized drops, which provide favorable conditions for quicker evaporation, better ignition, broader stability ranges, increased combustion efficiency, and reduced emissions of unburned hydrocarbons. The cone angle is also important because it affects atomizer dispersion behavior. For example, with increasing cone angles, there is increased fuel coverage area (more dispersion). More dispersion tends to lower fuel concentrations leading to lower emissions and less soot formation under lean combustion. If the cone angle, defined as "the angle formed by two straight lines drawn from the discharge orifice [10]," is small, spray characteristics approach those of a solid-cone spray, rather than the hollow-cone typical of a simplex atomizer. For narrow cone angles, the spray is dense and its penetration into the combustion chamber increases, which improves ignition and combustion stability at the expense of greater emissions for fuel-rich burning.

Basic simplex atomizer features (i.e., air core size, film thickness, cone angle, and discharge coefficient) are described in the pioneering analytical work of Taylor [13] and in later work by Taylor [14], Binnie and Harris [15], Giffen and Muraszew [16], Dombrowski and Hooper [17], Dombrowski and Johns [18,19], Dombrowski and Hasson [20], Clark and Dombrowski [21], Rizk and Lefebvre [22], Suyari and Lefebvre [23], and Yule and Chinn [24].

The effect of fluid physical properties (surface tension and viscosity) on atomizer performance is described by Dorfner et al. [25] and Stelter et al. [26]. Dorfner et al. concluded that the mean drop size increases as surface tension or viscosity increases. Lower

* Corresponding author. Tel.: +82 2 3290 3356; fax: +82 2 926 9290.
E-mail address: kimhy@korea.ac.kr (H.Y. Kim).

0894-1777/$ - see front matter © 2010 Elsevier Inc. All rights reserved.
doi:10.1016/j.expthermflusci.2010.07.010

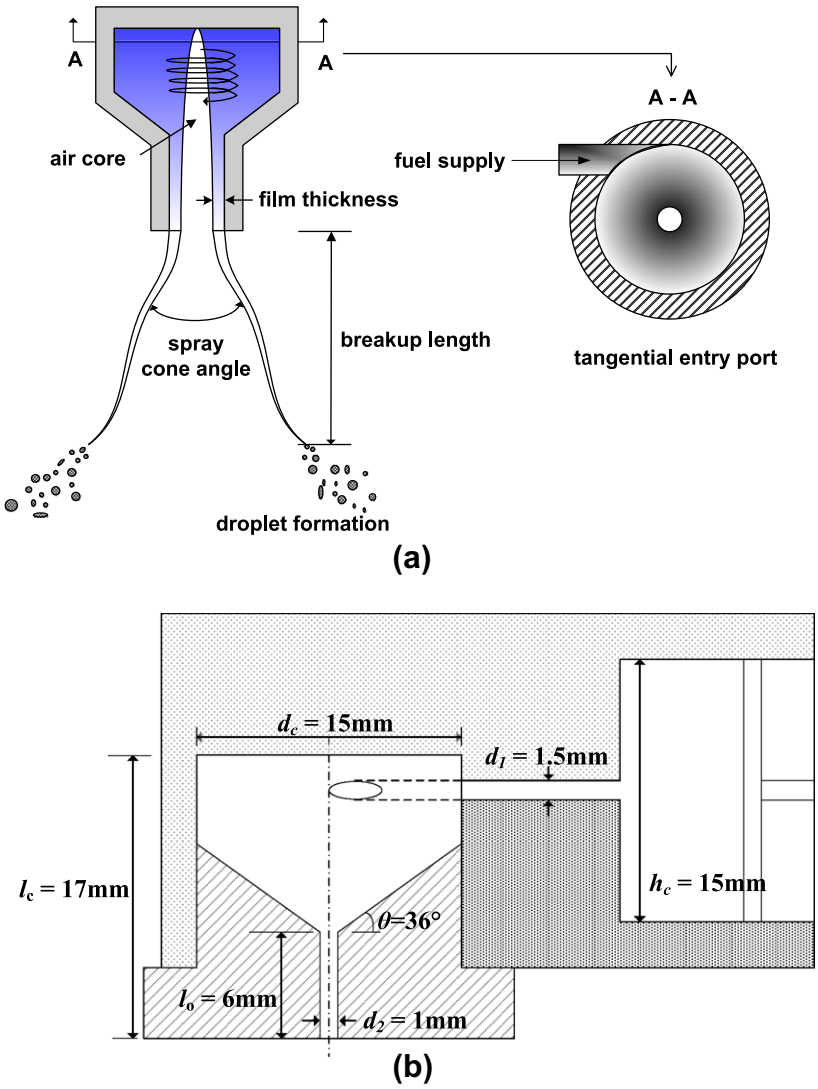

Fig. 1. (a) Schematic of a typical pressure-swirl atomizer. (b) The internal geometry of the pressure-swirl atomizer used in this study. All dimensions are in millimeters.

surface tension or viscosity results in narrower size distributions, tending toward monodisperse sprays. Stelter et al. [26] also evaluated the performance of a viscoelastic swirl spray, commonly used in agricultural and coating industries to avoid small drops that degrade atomizer performance because of drift effects caused by aerodynamic drag.

Predictions of initial conditions (i.e., drop size and velocity distributions) for a swirl spray are given by Cousin et al. [27], Boyaval and Dumouchel [28], Kim et al. [29], and Mondal et al. [30]. They all used the principle of maximum entropy to predict the mean drop size and distribution.

Fuel temperature is another important parameter that affects swirl-spray performance. During combustion, if fuel temperature is high (due to convective and radiative heat transfer from the compressor or the combustor during supersonic flight), improved atomization performance is observed because of increased specific energy and calorific value of the fuel, which in turn expedite evaporation. On the other hand, significant safety issues are associated with high-temperature fuel; see Refs. [31–36].

Conversely, the consequences of low fuel temperature are also rather dire. During high-altitude flight (i.e., cold environments), fuel temperature can drop as low as 230 K [35]. In such an environment, fuel is, at best, highly viscous, resulting in air core degradation. With weak swirl (either due to the high fuel viscosity or low injection pressure), an air core degrades or disappears. This begins as a transitional process where the jet pulsates and becomes unstable, resulting in poor atomization and combustion instability. Clearly, understanding the air core's behavior is important because it characterizes the stability of a swirl spray. In this work, we distinguish and report on three major regimes: First, "the unstable regime," where no air core is present inside a swirl chamber due to weak centrifugal force (significant pulsation of the external spray is observed); second, "the transitional regime," where an unstable air core is observed (spray outside the nozzle continues to fluctuate); and third, "the stable regime," where strong swirl ensures stability of the air core inside and produces high-quality atomization outside.

Though relevant work regarding air cores is presented by Som and Mukherjee [37], Datta and Som [38], Yule & Chinn [39], Dash et al. [40], Halder et al. [41], and Park et al. [42], our data are unique in that the regimes are distinctively categorized by the Reynolds number, which was changed by varying both the temperature (hence the kinematic viscosity) and pressure (hence fluid velocity) of diesel and a kerosene-based fuel, bunker-A. Note that the range of the operation conditions is 300–900 kPa and 283–363 K for pressure and fuel temperature, respectively. Also note

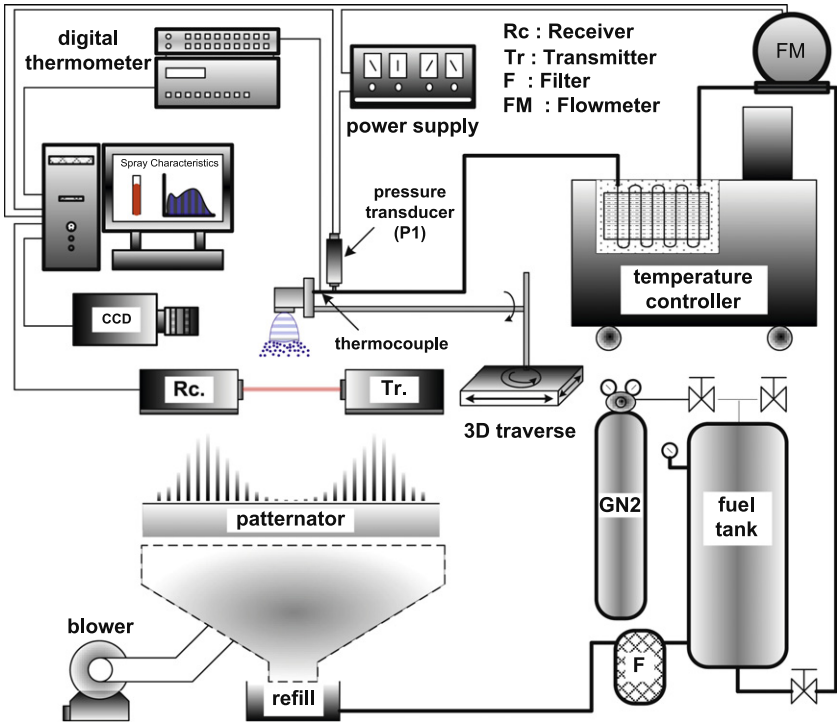

Fig. 2. Schematic of the experimental setup.

that the Reynolds number is defined as $Re = u_2 d_2/\nu$, where u_2 and d_2 are the velocity and inner diameter of the nozzle exit; $d_2 = 1.0$ mm; and ν is the kinematic viscosity of the fuel. u_2 is calculated using Bernoulli's equation; i.e., $u_2 = \sqrt{2(P_1 - P_2)/\rho_l}$, where P_1 is the injection pressure at the inlet/port indicated in Fig. 2 and ρ_l is the liquid density. The critical Reynolds numbers, which distinguish the aforementioned three regimes, are also reported. Next, an air core in the transitional regime is characterized and quantified. Finally, overall spray performances (i.e., SMD, cone angle, and discharge coefficient) are reported.

2. Experimental setup

2.1. Pressure-swirl atomizer

Fig. 1b is the schematic for the internal geometry of the pressure-swirl atomizer used in this experiment. The container of fuel ($h_c = 15$-mm height) was pressurized to force fuel through a tangential port into the swirl chamber ($d_c = 15$-mm diameter). There is only one tangential entry port in this atomizer, thus, the swirling strength is less than a similar multi-port swirl atomizer [22]. As the swirl develops inside the injector chamber, the fuel travels toward the nozzle in a helical pattern, undergoing a laminarization process through a converging nozzle, which provides a favorable pressure gradient. The converging angle within the swirl chamber is approximately 36°, and it is followed by a $l_o = 6$-mm-long, $d_2 = 1$-mm-diameter exit orifice length. A wall boundary layer develops, but the longer the nozzle orifice, the more likely it is that the flow is turbulent because of the unstable rollup motion of a thicker boundary layer [43]. An air core (a void column formed by the swirl's centrifugal force) is sustained at the center of the atomizer when it is working optimally.

2.2. Experimental apparatus

Fig. 2 is the schematic of the experimental apparatus. Fuel pressurized by nitrogen was driven through the submerged-bath heat exchanger to control its temperature before entering the atomizer. A pressure transducer and thermocouples were installed in the fuel supply pipe, located between the heat exchanger and the atomizer to measure the injection (or operating) pressure and the fuel temperature; uncertainties are within 1% for both pressure and temperature measurement according to the manufacturer's manual. The volumetric (or mass) flow rate was measured using a gear displacement flowmeter with accuracy better than 1%.

Three modules comprise the Malvern particle sizer: a transmitter, a receiver, and a computer. The transmitter included a 5-mW He–Ne laser emitted as an optical beam column, a 9-mm beam expander, and a 300-mm lens. The receiver contains a lens, detector, associated electronics, and computer interfaces. The Malvern measured the Sauter mean diameter (SMD) using Fraunhofer diffraction of a parallel beam of monochromatic light passing through the moving droplets. The dependence of the Malvern particle sizer on refractive indices is negligible for the particle size greater than 5 μm and the smallest SMD of our data is about 50 μm. This suggests that different fuel opacity (different refractive indices) does not significantly impact measurement accuracy for the flow regime we have explored. The diffraction patterns produced by the laser beam passing through the atomized droplets at various downstream locations were recorded and a Rosin–Rammler distribution was fit to the data. The SMD of the atomized droplets ranged from 50 to 200 μm with errors less than 5% according to previous experience [42]. The detector monitored the average value of the light scattering characteristics whose values were based on statistically reliable data sets (i.e., several million droplets).

The spray cone angle was measured 3 cm downstream from the atomizer tip using images captured with a CCD camera located about 1.2 m from the nozzle. The camera speed ranged from 500 to 10,000 fps. Front lighting was used with 1-kW illumination and the light was projected at a slightly oblique angle of 15°. The images obtained from the camera were transferred to a data-processing computer and used to measure the spray cone angle. A stroboscope illuminated the spray's dispersal pattern. The volume distribution of the atomizer was measured by a 1D patternator,

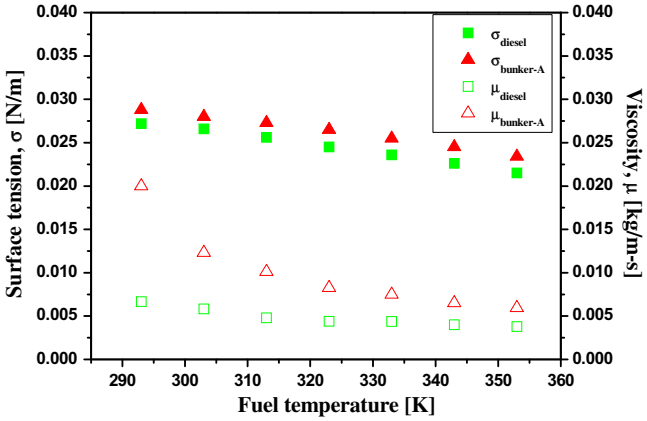

Fig. 3. Variation of the liquid properties (surface tension (N/m) and dynamic viscosity (kg/m-s)) with temperature for diesel and bunker-A.

consisting of 30 collecting bins connected to a refilling container that recycled collected fuel through the closed-loop fuel tank system.

2.3. Fuel properties

The fuels used in this study are diesel and a dark-colored, kerosene-based aviation fuel, bunker-A. Variations of the fuel viscosity and surface tension were experimentally measured and fit using the least squares technique. Viscosity and density were measured using a digital viscometer (*DV-2 + PRO, BROOKFIELD, USA*), whose accuracy lies within 1% of full scale range. Surface tension was measured using a surface tensiometer (*CBVP-A3, FACE, Japan*), whose accuracy lies within 0.2 dyne/cm. The regression fits to these data are shown in Fig. 3, and the least squares approximations are:

$$\begin{aligned}
\mu_{\text{diesel}} &= 409.81\exp\left(-\frac{T}{24.87}\right)+0.0036,\\
\mu_{\text{Bunker-A}} &= 6.93\times10^{6}\exp\left(-\frac{T}{14.61}\right)+0.0062,\\
\sigma_{\text{diesel}} &= -0.0038\exp\left(-\frac{T}{199.17}\right)+0.044,\\
\sigma_{\text{Bunker-A}} &= -5.05\times10^{-4}\exp\left(-\frac{T}{109.40}\right)+0.036,
\end{aligned} \tag{1}$$

where μ and σ represent dynamic viscosity and surface tension, respectively, for diesel and bunker-A. For bunker-A, there is a rapid increase in viscosity in the low-temperature region eventually resulting in poor (or no) performance from the simplex atomizer. The surface tension of the fuel also increases at low temperatures, even though its rate of change less than viscosity's.

3. Results and discussion

3.1. Air core

Fig. 4 (left column) shows snapshots of the atomizing diesel spray at various injection pressures. Fig. 4 (right column) shows the time variation of injection pressure and the volumetric flow rate at the nozzle exit. It should be noted that the nominal pressure P_1 is measured at the nozzle inlet port. The swirl chamber, made of a transparent acryl-based material, is shown, but the air core is difficult to distinguish in these snapshots. At relatively low pressure (e.g., 0.3 MPa), the data (recorded at a rate of 879/s) indicate that flow rate fluctuation is moderate; however, the external spray fluctuated visually. The air core is not present in this unstable regime due to weak swirl, which also means that atomized fuel does not acquire strong radial velocity and a relatively small cone angle results. The hollow-cone pattern typical of a swirl atomizer more closely resembles a solid-cone spray. In this unstable regime, turbulence likely interrupts the helical flow in the swirl chamber. The transitional regime appears upon increasing the pressure to 0.5 MPa; the air core starts to form. The swirl strength is still low in this regime and thus, the shape and height of the air core are unstable. The measured pressure and flow rate are also notably unstable in this transitional regime. With sufficient swirl at high pressure (e.g., 0.9 MPa), the air core fills the entire length of the chamber; the external spray is stable and its atomization quality is optimal.

Fig. 5 (left column) shows snapshots of the atomizing spray at various injection pressures; illustrating the three regimes. Bunker-A is dark and non-transparent and the presence of the air core could not be visually verified. Fig. 5 (right column) shows the time variations of injection pressure and volumetric flow rate at the nozzle exit.

Fig. 6 shows the measured air core length, varying due to injection pressure and fuel temperature changes for diesel. Regions *A*, *B–D*, and *E* represent the unstable, transitional, and stable regimes, respectively. In Region *B*, beginning at $Re \approx 2550$, the air core fluctuates wildly, ranging in normalized length (air core length, l_a divided by the chamber length, l_c) from 0.10 to 0.35. In Region *C*, the air core is still in the transitional stage, but its normalized length is relatively stable at 0.38. Minor fluctuations are still observed in Region *D* between 0.38 and 0.42. Once past Region *D*, a sudden jump takes place to Region *E*, where the normalized air core length goes from $l_a/l_c = 0.42$ to unity and complete stability. This critical change occurs at the $Re \approx 3450$ for diesel. It is noteworthy that the air core length is comparable to the orifice length $l_o/l_c = 0.353$ at the critical Reynolds number. In the orifice (contracted/laminarized region), the air core fluctuates because swirl motion is weaker under tangential speeds, given the small orifice radius ($d_2/2$). In the upper portion of the chamber, tangential speed is higher because of the larger chamber diameter (d_c) and this facilitates a more stable swirl motion of the air core. The air core length for bunker-A could not be measured because of fuel opacity.

3.2. Sauter mean diameter

The SMD of diesel, recorded at center and off-center locations (i.e., $R = 0$, 1, and 2 cm), are shown in Fig. 7; the axial location distance was at 9 cm below the nozzle exit. SMD decreases with increasing *Re* for both diesel and bunker-A. Relatively larger droplets are observed at increasing radial distances because larger droplets tend to travel farther due to their greater momentum. A gradation of particle sizes in the radial direction is seen due to different dynamic behavior of small and large particles. Large particles are dispersed by the spray initial cone angle and subsequent interactions with turbulent eddies in the entrained air, while smaller particles are generally increasingly swept toward the spray centerline by aerodynamic drag interactions with the entrained air [44].

It was previously mentioned that Dorfner et al. [25] found that SMD increased with increasing viscosity and surface tension. Contrarily, we found that the SMD for bunker-A is slightly smaller than that for diesel despite viscosity and surface tension of bunker-A being greater than those of diesel's (at the same *Re*). Because bunker-A viscosity is greater than that of diesel, the corresponding velocity (at the nozzle exit) should be greater for bunker-A than for diesel at the same *Re*. The increased exit velocity for bunker-A is achieved by increasing the operating/injection pressure, ΔP. Given that all SMD data shown in Fig. 7 are obtained by varying

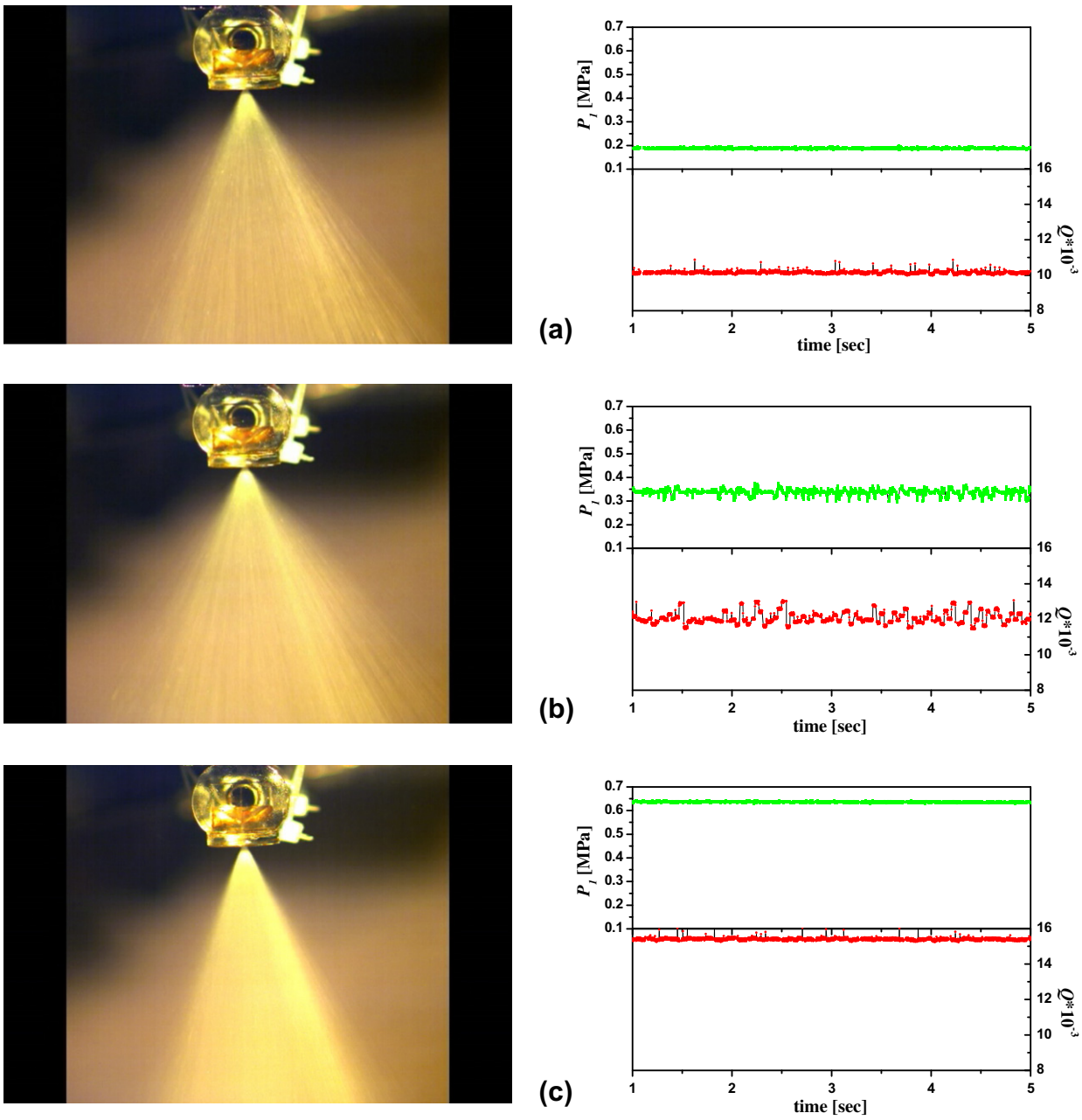

Fig. 4. Diesel: snapshots (left) of the three regimes and their time variation in injection pressure (green curves) and flow rate (red curves) at T = 293 K (right). (a) Unstable regime at ΔP = 0.3 MPa, (b) transitional regime at ΔP = 0.5 MPa, and (c) stable regime at ΔP = 0.9 MPa. The units for pressure (P_1) and volumetric flow rate (Q) are in (MPa) and [l/s], respectively. The explored range of the operating condition for the diesel case is 300–900 kPa and 283–313 K for pressure and fuel temperature, respectively. See Fig. 8 for the cone angle as a function of *Re*. (For interpretation of the references to colour in this figure legend, the reader is referred to the web version of this article.)

both the injection pressure and fuel's temperature (T), SMD is a function of both ΔP and T. However, SMD is more strongly affected by ΔP than by T. Thus, at the same *Re*, ΔP is greater for bunker-A, which in turn yields a slightly smaller SMD than diesel.

3.3. Cone angle

The cone angle is another important parameter that characterizes the performance of a simplex atomizer. Recall that the cone angle is a measure of dispersion quality affecting spray penetration, ignition, combustion stability, and emission levels. For Gasoline Direct Injection engines, an optimum cone angle yields a stable combustion process, imparting maximum engine torque with minimum emissions. The cone angle is defined as the angle formed between two straight lines drawn along the spray from the nozzle exit (see Fig. 1). The cone angle is controlled by the internal geometry and size of the nozzle (i.e., port, chamber, and orifice diameters) and also by aerodynamic influences (i.e., entrainment and air density). Previous inviscid theories [14–16] and other empirical data [22] offer analytic and empirical predictions for cone angle as a function of these geometric and fluid parameters.

In our experiment, the cone angle is controlled by varying the injection pressure and fuel temperature, which also vary *Re*. Because of fluctuations in the cone angle, both maximum and minimum values are recorded; their differences are indicated with green triangles in Fig. 8. In the stable regime, an increase in *Re*

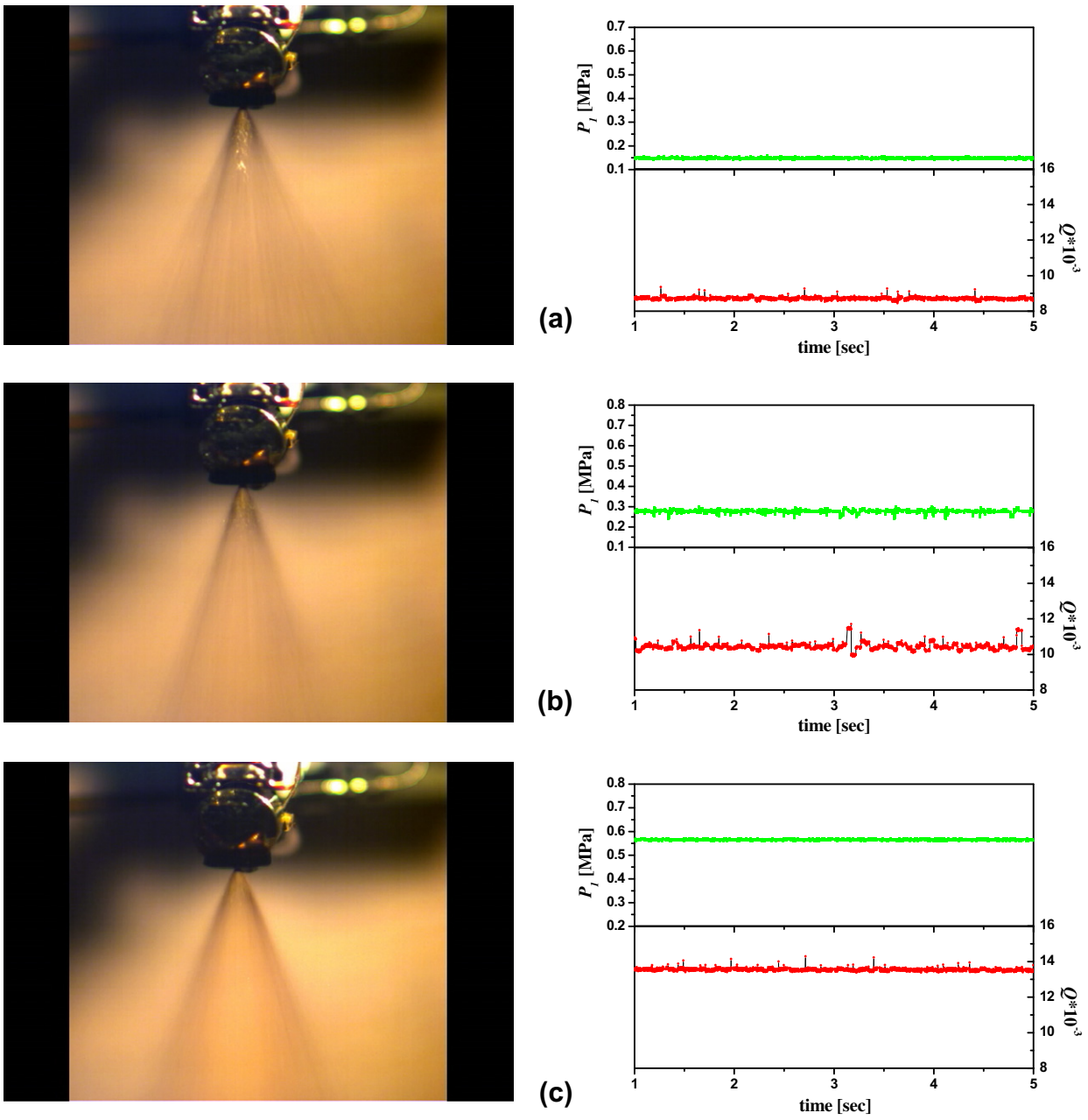

Fig. 5. Bunker-A: snapshots (left) of the three regimes and their time variation in injection pressure (green curves) and flow rate (red curves) at T = 358 K (right). (a) Unstable regime at ΔP = 0.3 MPa, (b) transitional regime at ΔP = 0.5 MPa, and (c) stable regime at ΔP = 0.9 MPa. The units for pressure (P_1) and volumetric flow rate (Q) are in (MPa) and (l/s), respectively. The explored range of the operating condition for the bunker-A case is 300–900 kPa and 323–363 K for pressure and fuel temperature, respectively. (For interpretation of the references to colour in this figure legend, the reader is referred to the web version of this article.)

yields an increase in cone angle from 45° to 60° and there is little difference between maximum and minimum cone angles. Differences are significant in Regions *A* and *B* (the unstable and transitional regimes).

Fig. 9 shows the cone angle variation for bunker-A. At low *Re* (around 1500), the cone angle is minimum because there is essentially no swirl. At around *Re* = 1650, a sudden increase in the cone angle is observed, but its range fluctuates until stable Region E is achieved at around *Re* = 3300. Data are available up to *Re* = 3450; further increasing *Re* for bunker-A was impossible due to pressure-vessel limitations. Although analytical and empirical relations for the cone angle are available [14,15,20,23], direct comparison is not possible because their swirl-port design significantly differs from the design used in these experiments.

3.4. Discharge coefficient

The discharge coefficient is defined as the ratio between actual and theoretical flow rates. It represents the ratio between the spray's flow rate with an ideal air core to the actual flow rate:

$$C_D = \frac{\dot{m}_{act}}{\dot{m}_{th}} = \frac{\dot{Q}_{act}}{\dot{Q}_{th}} = \frac{u_{act}}{u_2}\left[1 - \left(\frac{D_{aircore}}{D_2}\right)^2\right], \text{ where}$$

$$u_2 = \sqrt{\frac{2(P_1 - P_2)}{\rho}}, \tag{2}$$

Here, the actual exit velocity (u_{act}) is always less than the theoretical exit velocity (u_2), obtained using the inviscid Bernoulli equation because of friction losses. Even for an inviscid fluid, the

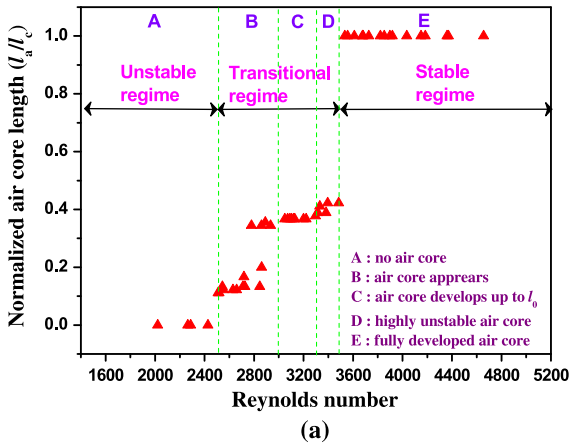

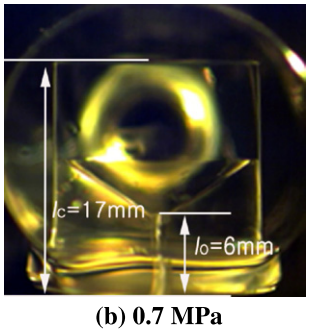

Fig. 6. (a) Diesel air core length, normalized by the chamber length (17 mm), in the three regimes as a function of *Re*. The explored range of the operating condition for the diesel case is 300–900 kPa and 283–313 K for pressure and fuel temperature, respectively. (b) Image of an air core and nozzle chamber length at operating condition for an injection pressure of 0.7 MPa.

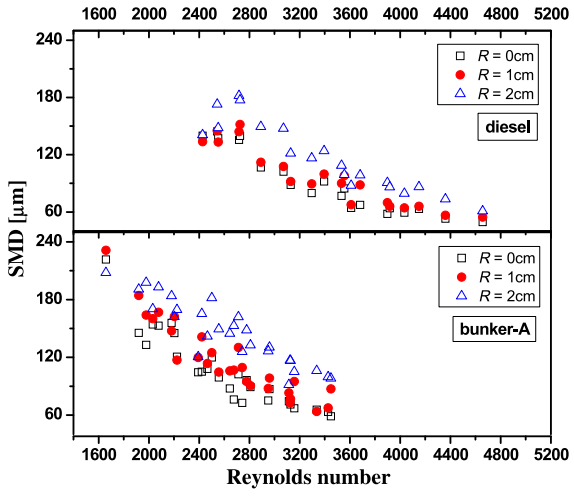

Fig. 7. SMD vs. *Re* at various radial locations for diesel and bunker-A.

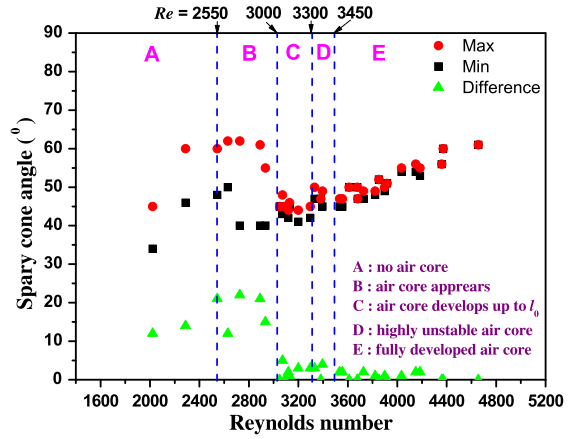

Fig. 8. Spray cone angle vs. *Re* for diesel.

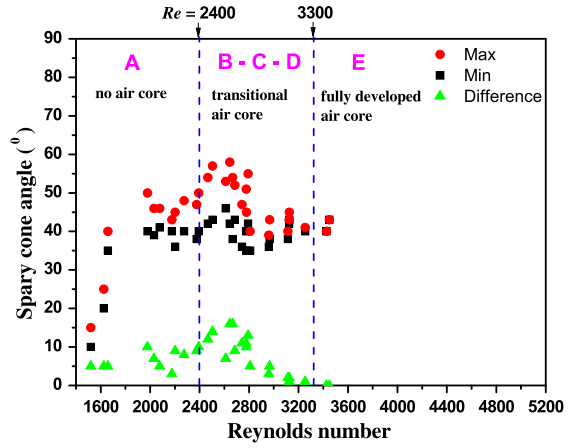

Fig. 9. Spray cone angle vs. *Re* for bunker-A.

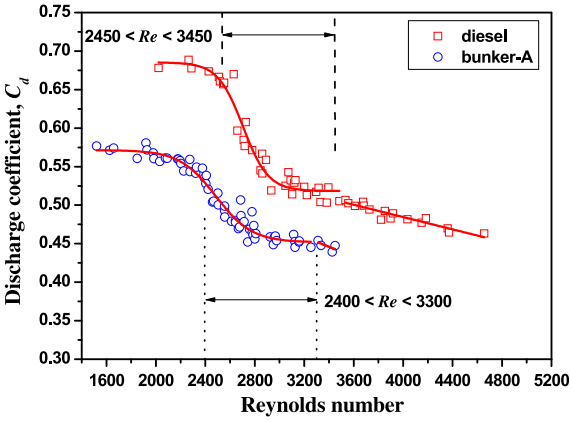

Fig. 10. Discharge coefficients as a function of *Re* for diesel and bunker-A.

air core itself reduces the discharge coefficient, thus only for an inviscid flow with no air core could the discharge coefficient be one. Typically, increasing the port velocity (by decreasing the port area) at a given injection pressure causes the discharge coefficient to decrease. Upon increasing the port velocity (hence increasing the exit velocity) [22], a thinner liquid film should be formed in the chamber and the air core should grow. Once in the stable regime, the discharge coefficient becomes insensitive to *Re*; the cone angle and flow rate reach maximum values and no further increase in radial velocity of sprayed droplets is achievable. These expected responses are demonstrated in Fig. 10. There are steep negative slopes between $2550 < Re < 3450$ and $2400 < Re < 3300$ for diesel and bunker-A, respectively. In a previous study, this steep negative slope was observed for $2500 < Re < 3500$ for kerosene-based fuels [42]. The negative slope is indicative of the formation of an air core during the transitional regime while increasing *Re*. The differences in *Re* between the previous and current studies is likely due to a different surface roughness (different nozzle materials) and different thermo-physical properties of the working fluid.

As the air core stabilizes, the fuel's volumetric (or mass) flow rate reduces as the center of the injector is increasingly occupied by the air core; hence the reduction in discharge coefficient. The data fit the following empiricisms in the nonlinear region:

$$\begin{aligned} C_d &= 0.52 + \frac{0.17}{1 + 10^{-0.00.425(2705 - Re)}} : \text{diesel}, \\ &= 0.45 + \frac{0.12}{1 + 10^{-0.00296(2484 - Re)}} : \text{bunker -A}. \end{aligned} \tag{3}$$

In the linear region, the discharge coefficients are:

$$\begin{aligned} C_d &= 0.64 - 4.00 \times 10^{-5} \times Re \quad : \text{diesel}, \\ &= 0.66 - 6.21 \times 10^{-5} \times Re \quad : \text{bunker-A}. \end{aligned} \tag{4}$$

4. Conclusion

Flow characteristics of a pressure-swirl atomizer were conducted for various fuel temperatures and injection pressures. The working liquids were diesel and a kerosene-based aircraft fuel, bunker-A, which is more viscous and has greater surface tension than diesel. Poorer atomization performance was observed for bunker-A than for diesel. We characterized how at low injection pressures or/and fuel temperatures, the atomizer loses its distinctive swirl and exhibits unstable fuel spray patterns. Using an acryl-based, transparent nozzle, the length of the air core (for diesel) was measured as a function of *Re*, which was varied by changing the injection pressure and fuel temperature. The critical Reynolds numbers, which identify regime changes from unstable to transitional (and eventually to the stable) modes, were also reported. The regimes were categorized as: (1) the unstable regime, where no air core was present inside the swirl chamber due insufficient centrifugal forces (significant pulsation of the external spray was observed); (2) the transitional regime, where an unstable air core was observed (spray from the nozzle continued to fluctuate); and (3) the stable regime, where a strong swirl ensured stability of the air core and produced high-quality atomized spray. For diesel, the air core first appeared at $Re \approx 2550$, indicating the onset of the transitional regime where the air core fluctuated wildly, ranging in normalized length from $l_a/l_c = 0.10$ to 0.43. The air core for bunker-A could not be visually verified because of its dark, opaque color. There are steep negative slopes for the discharge coefficient for $2550 < Re < 3450$ and $2400 < Re < 3300$ for diesel and bunker-A, respectively, that delineate the transitional regime. A fully developed air core was observed for diesel when $Re > 3450$ and spray cone angle data suggest the same for bunker-A when $Re > 3300$. Our studies suggest that for low operating temperatures, pressure-swirl atomizer pressures should be increased to ensure optimum fuel atomization and dispersal.

Acknowledgements

This research was supported by a grant from Development of Engine System for HEV Project, funded by the Ministry of Knowledge Economy. The last author acknowledges that this study was partially supported by a grant from the cooperative R&D Program (B551179-08-03-00) funded by the Korea Research Council Industrial Science and Technology and also by KETEP (2009-3021010030-11-1).

References

[1] D.H. Huntington, The influence of the spray drying process on product properties, Dry. Technol. 22 (2004) 1261–1287.
[2] B.Q. Li, T. Cader, J. Schwarzkopf, K. Okamoto, B. Ramaprian, Spray angle effect during spray cooling of microelectronics: experimental measurements and comparison with inverse calculations, Appl. Therm. Eng. 26 (2006) 1788–1795.
[3] G.G. Nasr, R.A. Sharief, A.J. Yule, High pressure spray cooling of a moving surface, J. Heat Transfer 128 (2006) 752–760.
[4] F. Zhao, M.C. Lai, D.L. Harrington, Automotive spark ignited direct injection gasoline engines, Prog. Energy Combust. Sci. 25 (1999) 437–562.
[5] J.M. Nouri, J.H. Whitelaw, Spray characteristics of a gasoline direct injector with short durations of injection, Exp. Fluids 31 (2001) 377–383.
[6] R. Rontondi, G. Bella, Gasoline direct injection spray simulation, Int. J. Therm. Sci. 45 (2006) 168–179.
[7] N.B.H. Abdelkarim, S.S. Ibrahim, A.R. Masri, G. Wigley, Gasoline sprays injected at different back pressures: calculations using two atomization models, Atomization Sprays 17 (2007) 233–265.
[8] A. Singh, M. Mehregany, S.M. Phillips, R.J. Harvey, M. Benjamin, Micromachined silicon fuel atomizers for gas turbine engines, Atomization Sprays 8 (1998) 405–418.
[9] H. Alkabie, Design methods of the ABB ALSTOM POWER gas turbine dry low emission combustion system, Proc. Inst. Mech. Eng. 214 (A) (2000) 293–315.
[10] A. Lefebvre, Fifty years of gas turbine fuel injection, Atomization Sprays 10 (2000) 251–276.
[11] W.S. Rayleigh, On the instability of cylindrical fluid surfaces, Philos. Mag. 34 (1892) 207.
[12] J. Ponstein, Instability of rotating cylindrical jets, Appl. Sci. Res. 8 (1959) 425–456.
[13] G.I. Taylor, The mechanics of swirl atomizers, 7th Int. Cong. Appl. Mech. 1 (1948) 280–285.
[14] G.I. Taylor, The boundary layer in the converging nozzle of a swirl atomizer, Q. J. Mech. Appl. Mech. 3 (1950) 129–139.
[15] A.M. Binnie, D.P. Harris, The application of boundary-layer theory to swirling liquid flow through a nozzle, Q. J. Mech. Appl. Mech. 3 (1950) 89–106.
[16] E. Giffen, A. Muraszew, Atomization of Liquid Fuels, Chapman & Hall, London, 1953.
[17] N. Dombrowski, P.C. Hooper, The effect of ambient density on drop formation in sprays, Chem. Eng. Sci. 17 (1962) 291–305.
[18] N. Dombrowski, W.R. Johns, The aerodynamic instability and disintegration of viscous liquid sheets, Chem. Eng. Sci. 18 (1963) 203–214.
[19] N. Dombrows, W.R. Johns, Thermal properties of combustion gases from a residual fuel–oil fired high intensity combustion chamber, J. Inst. Fuel 42 (1969) 194–199.
[20] N. Dombrowski, D. Hassan, The flow characteristics of swirl centrifugal spray pressure nozzles with low viscosity liquids, AIChE J. 15 (1969) 404.
[21] C.J. Clark, N. Dombrowski, Aerodynamic instability and disintegration of inviscid liquid sheets, Proc. Roy. Soc. London Ser. A Math. Phys. Sci. 329 (1972) 467–478.
[22] N.K. Rizk, A.H. Lefebvre, Internal flow characteristics of simplex swirl atomizers, J. Propul. Power 1 (1985) 193–199.
[23] M. Suyari, A.H. Lefebvre, Film thickness measurements in a simplex swirl atomizer, J. Propul. 2 (1986) 528–533.
[24] A.J. Yule, J.J. Chinn, Swirl atomizer flow: classical inviscid theory revisited, in: Sixth International Conference on Liquid Atomization and Spray Systems, Rouen, France, 1994, pp.334–341.
[25] V. Dorfner, J. Domnick, F. Durst, R. Kohler, Viscosity and surface tension effects in pressure swirl atomization, Atomization Sprays 5 (1995) 261–285.
[26] M. Stelter, G. Brenn, F. Durst, The influence of viscoelastic fluid properties on spray formation from flat-fan and pressure-swirl atomizers, Atomization Sprays 12 (2002) 299–327.
[27] J. Cousin, S.J. Yoon, C. Dumouchel, Coupling of classical linear theory and maximum entropy formalism for prediction of drop size distribution in sprays: application to pressure-swirl atomizers, Atomization Sprays 6 (1996) 601–622.
[28] S. Boyaval, C. Dumouchel, Investigation on the drop size distribution of sprays produced by a high-pressure swirl injector: measurements and application of the maximum entropy formalism, Part. Part. Syst. Charact. 18 (2001) 22–49.
[29] W.T. Kim, S.K. Mitra, X. Li, L.A. Prociw, T.C.J. Hu, A predictive model for the initial droplet size and velocity distributions in sprays and comparison with experiments, Part. Part. Syst. Charact. 20 (2003) 135–149.
[30] D. Mondal, A. Datta, A. Sarkar, Prediction of drop size distribution in a spray from a pressure swirl atomizer using maximum entropy formalism, Proc. Inst. Mech. Eng. 217 (2003) 831–838.
[31] E.A. Droegemueller, Fuel requirements for supersonic, Esso Air World 16 (1963) 2.
[32] W.G. Dukek, A short history of thirty years of jet fuel, Esso Air World 22 (1969) 3.
[33] W.D. Sherwood, Shell Aviation News, 1965.
[34] J.P. Longwell, Prog. Astronaut. Aeronaut. 62 (1978) 3.
[35] X.F. Wang, A.H. Lefebvre, Influence of fuel temperature on atomization performance of pressure-swirl atomizers, J. Propul. Power 4 (1988) 222–227.
[36] A. Demirbas, The influence of temperature on the yields of compounds existing in bio-oils obtained from biomass samples via pyrolysis, Fuel Proc. Technol. 88 (2007) 591–597.
[37] S.K. Som, S.G. Mukherjee, Theoretical and experimental investigations on the formation of air core in a swirl spray atomizing nozzle, Appl. Sci. Res. 26 (1980) 173–196.
[38] A. Datta, S.K. Som, Numerical prediction of air core diameter, coefficient of discharge and spray cone angle of a swirl spray pressure nozzle, Int. J. Heat Fluid Flow 21 (2000) 412–419.
[39] A.J. Yule, J.J. Chinn, The Internal flow and exit conditions of pressure swirl atomizers, Atomization Sprays 10 (2000) 121–146.

[40] S.K. Dash, M.R. Halder, M. Peric, S.K. Som, Formation of air core in nozzles with tangential entry, J. Fluids Eng. 123 (2001) 829–835.
[41] M.R. Halder, S.K. Dash, S.K. Som, Initiation of air core in a simplex nozzle and the effects of operating and geometrical parameters on its shape and size, Exp. Therm. Fluid Sci. 26 (2002) 871–878.
[42] B.S. Park, H.Y. Kim, S.S. Yoon, Transitional instability of a pressure-swirl atomizer due to air core eruption at low temperature, Atomization Sprays 17 (2007) 551–568.
[43] H. Schlichting, Boundary Layer Theory, McGraw-Hill Inc., 1960.
[44] S.S. Yoon, J.C. Hewson, P.E. DesJardin, D.J. Glaze, A.R. Black, R.R. Skaggs, Numerical modeling and experimental measurements of a high speed solid-cone water spray for use in fire suppression applications, Int. J. Multiphase Flow. 30 (2004) 1369–1388.